

# Acknowledgment

本研究之得以順利完成，首先感謝柯博的指導與信任，以及對於研究成果悉心校閱與指正。謝謝佳典學長一開始對於初到新竹的我的照顧，以及研究上的指導與支持。感謝其昌學長、俊淇學長、銘清學長在研究上不吝給我意見與協助。

終於畢業了！我要謝謝皮皮那段日子的陪伴與鼓勵，謝謝你的簡訊與安慰的話，沒有你也許不會有今天。有段時間每天到實驗室最期待的就是和你分享有什麼好貨互相交換心得或生活中的趣事，真是很懷念。。。我很珍惜這一段緣份。謝謝吳中書的細心，我傷心難過的時候你會發現，會關心我開導我。謝謝你總是願意伸出援手。你是安定的力量。謝謝鄭捷，雖然有時候我們有摩擦，但謝謝你不論實驗或生活中給我的建議與幫助，你也總是觀察入微給我適時的關心。有阿生在的日子就有吃吃喝喝與歡笑，很想念你的 Honda 停在工一的時光。謝謝依臻總是默默的付出，不懂的地方向你請教你都會盡力教我。也謝謝小花，有許多電腦上不懂的問題都要麻煩你，你有好吃好玩的也都會和我分享，謝啦！

謝謝玟菲、京彰、柏軒在實驗上給我的幫助，有不會的地方你們總是不厭其煩的告訴我，機台儀器也有許多麻煩你們的地方，謝謝。也感謝實驗室一群可愛各有特色的學弟妹：丁香的熱心付出，易成的專業與認真，崇志的善良好相處，小丁對物理的熱誠，品樺的努力與善良，有你們在實驗室熱鬧許多。

謝謝 physics 在我遇到問題與面臨人生的轉折時給我的幫助與建議，衷心感謝你。謝謝胖子的支持與鼓勵，在我沮喪時給我力量。感謝機械幫的大家，聚會時互相吐苦水分享彼此的生活為對方加油打氣，有你們在新竹變得不那麼陌生。

另外要謝謝郭宇彥學長與吳志力學長，謝謝你們的幫助，在實驗遇到困難時願意花時間幫助我。

謝謝 S' Ma 在我遇到困難竭盡所能的幫助我，在碰到挫折時聽我訴苦安慰我，陪我一起熬夜趕論文，幫我處理許多問題（其實你才是 Apple 的受害者吧），謝謝有你。

最後要謝謝我的家人，感謝你們的付出與關愛，讓我終於順利完成學位。我要對我最愛的母親說聲：媽，謝謝你。

以孔洞氧化鋁自組裝二氧化鈦空心半球  
伴隨二氧化鈦奈米管陣列  
應用於染敏太陽能電池

學生：何嘉琦

指導教授：柯富祥

國立交通大學

奈米科技研究所



摘 要

近年來，染料敏化太陽能電池在再生能源範疇引起廣泛的討論與高度注意。具有高表面積的電極以利染料吸附並獲取更多光子為高效率染敏太陽能電池必需的條件。為了達到此目的，許多團隊致力於電極結構的改良與研發。

利用填充二氧化鈦前驅物入陽極氧化鋁管壁以形成二氧化鈦奈米管，在應用於染敏太陽能電池上展示許多優點。二氧化鈦奈米管沿著陽極氧化

鋁管壁生成，藉由陽極氧化鋁管壁的阻隔可有效防止二氧化鈦奈米管互相接觸而延遲電子傳輸，由此可提升電池效率。此外，陽極氧化鋁可防止電子與電解液中電洞再結合的發生。然而陽極氧化鋁與導電玻璃界面間的接合一直是各研究團隊所遭遇到的問題。

許多研究著重在一維二氧化鈦材料用於電極的開發，然而至今仍少有結合一維與空心結構的電極提出。我們團隊提出-陽極氧化鋁模板自組裝二氧化鈦奈米空心半球伴隨二氧化鈦奈米管陣列這樣的結構作為染敏太陽能電池電極。藉由沈積一層鈦於導電玻璃上可增進導電玻璃與鋁的接觸並利於後續的陽極氧化進行。陽極氧化過程中，當上方的鋁已形氧化鋁並反應至下方的鈦，此時二氧化鈦奈米空心半球自發生成。

自主裝二氧化鈦奈米空心半球高約 130 奈米，寬約 200 奈米。利用二氧化鈦前驅物  $Ti(OC_3H_7)_4$  形成之二氧化鈦奈米管陣列管徑寬 200 奈米，長 700 奈米垂直生長於導電玻璃上方，並經確認為銳鈦礦。在經過後續的四氯化鈦處理可增加結構表面積進而提升電池效率。陽極氧化鋁模板自組裝二氧化鈦奈米空心半球伴隨二氧化鈦奈米管陣列作為染敏太陽能電池電極，可達到短路電流  $5.00 \text{ mA/cm}^2$ ，開路電壓  $0.58 \text{ V}$ ，效率為傳統利用奈米粒子為電極電池的 1.77 倍。

# **Self-Organized Hollow TiO<sub>2</sub> Hemispheres under Porous Alumina with TiO<sub>2</sub> Nanotubes inside Applied in Dye-Sensitized Solar Cells**

Student: Chia-Chi Ho

Advisor: Dr. Fu-Hsiang Ko

Institute of Nanotechnology  
National Chiao Tung University



## **Abstract**

Dye-sensitized solar cells (DSSCs) have attracted extensive interest in past decade as a promising candidate for the future generation of cost-effective photovoltaic solar cells. It is well-accepted that a high efficiency photoelectrode for DSSCs requires a high surface area for light harvesting. To satisfy this requirement, much effort has motivated recently in development of electrode geometry.

TiO<sub>2</sub> nanotubes using anodic aluminum oxide (AAO) to backfill the template with TiO<sub>2</sub> precursor showed a lot of advantages in DSSC application. TiO<sub>2</sub> nanotubes are formed along the channels and separated by isolation alumina. The divided nanotubes without interconnections improve electron transport leading to higher photoefficiencies; plus, the alumina layer slows the recombination of the photo-generated electrons on the TiO<sub>2</sub> conduction band and holes in the electrolyte or the oxidized dye. However, the poor contact between FTO (fluorine-doped tin oxide) and AAO may cause a serious leakage of electron transport.

While considerable studies have focused on the preparation of 1D TiO<sub>2</sub>, no methods have

been available to combine those with hollow structures. We introduce a novel photoelectrode architecture consisting of self-organized hollow TiO<sub>2</sub> hemispheres under porous alumina with TiO<sub>2</sub> nanotubes inside. By depositing a thin layer of Ti on FTO substrates before anodization, we improve the contact between FTO substrates and overlaying aluminum; meanwhile, when the aluminum layer is consumed up to the underlying Ti, growth of hollow TiO<sub>2</sub> hemispheres under the bottoms of the alumina pores spontaneously occurred.

The self-organized hollow TiO<sub>2</sub> hemisphere with a height of 130 nm and a diameter of 200 nm was formed. Highly ordered TiO<sub>2</sub> nanotube arrays of 200-nm pore diameter and 700-nm length were grown perpendicular to a FTO substrate by infiltrating the alumina pores with Ti(OC<sub>3</sub>H<sub>7</sub>)<sub>4</sub> which was subsequently converted into anatase TiO<sub>2</sub>. The structure was treated with TiCl<sub>4</sub> to enhance the photogenerated current and then integrated into the DSSC using a commercially available ruthenium-based dye. The dye-sensitized solar cell using self-organized hollow TiO<sub>2</sub> hemispheres under porous alumina with TiO<sub>2</sub> nanotubes inside as the working electrode generated a photocurrent of 5.00 mA/cm<sup>2</sup>, an open-circuit voltage of 0.58 V and yielding a power conversion efficiency 1.77 times the conventional nanoparticle-based DSSC.

# Contents

Acknowledgment-----	I
Chinese Abstract-----	II
Abstract-----	IV
Contents-----	VI
List of Tables-----	VIII
List of Figures-----	IX
<b>Chapter 1: Introduction.....</b>	<b>1</b>
1.1 General Introduction .....	1
1.2 Dye-Sensitized Solar Cell.....	4
1.2.1 Construction.....	5
1.2.2 Working Mechanisms.....	10
1.2.3 Photovoltaic Performance.....	11
<b>Chapter 2: Literatures Review.....</b>	<b>14</b>
2.1 Nanoparticle-Based DSSC.....	14
2.2 Nanowire-Based DSSC.....	16
2.3 Nanotube-Based DSSC.....	19
2.4 Anodic Aluminum Oxide (AAO) Applied in DSSC.....	23
2.5 Hollow Sphere-Based DSSC.....	27
2.6 Motivation.....	31



<b>Chapter 3: Experiment.....</b>	<b>34</b>
3.1 General Introduction.....	34
3.2 Syntheses of Nanostructure Electrodes.....	36
3.2.1 Anodic Aluminum Oxide Fabrication.....	38
3.2.2 TiO <sub>2</sub> Sol-Gel Process.....	39
3.2.3 TiCl <sub>4</sub> Treatment.....	40
3.2.4 Counter Electrodes.....	41
3.3 Dye Sensitized and Cell Assembled.....	41
3.4 Materials Characterization.....	42
<b>Chapter 4: Results and Discussion.....</b>	<b>44</b>
4.1 Anodization Behavior of Aluminum on FTO Glass.....	44
4.2 Electrode Morphology Analysis.....	46
4.2.1 FTO Glass Surface Analysis.....	46
4.2.2 Self-Organized Hollow TiO <sub>2</sub> Hemispheres under Porous Alumina .....	48
4.2.3 TiO <sub>2</sub> Nanotubes.....	51
4.2.4 Influence of TiCl <sub>4</sub> Treatment.....	56
4.3 Mechanism of growth of Self-Organized Hollow TiO <sub>2</sub> Hemispheres	59
4.4 Photoelectric Characterization.....	60
4.4.1 I-V Characteristics.....	60
4.4.2 TiCl <sub>4</sub> Processed DSSC.....	65
<b>Chapter 5: Conclusions.....</b>	<b>68</b>

**References..... 69**

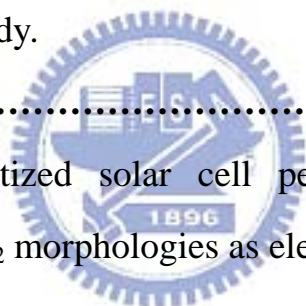
## List of Tables

**Table 1-1..... 3**  
Photovoltaic conversion efficiencies.

**Table 2-1..... 17**  
Comparison of electron mobilities ( $\text{cm}^2 \text{V}^{-1} \text{s}^{-1}$ ) of 1-D nanomaterials and nanoparticles.

**Table 3-1..... 36**  
The materials used in this study.

**Table 4-1..... 65**  
Summary of the dye-sensitized solar cell performance metrics for cells constructed with various  $\text{TiO}_2$  morphologies as electrodes.





# List of Figures

<b>Figure 1.1</b> .....	<b>1</b>
Historical and projected world energy supply and demand.	
<b>Figure 1.2</b> .....	<b>2</b>
Worldwide primary energy consumption by energy type.	
<b>Figure 1.3</b> .....	<b>5</b>
The construction of dye-sensitized solar cell.	
<b>Figure 1-4</b> .....	<b>7</b>
Band positions of several semiconductors in contact with aqueous electrolyte at pH 1.	
<b>Figure 1-5</b> .....	<b>8</b>
Structure of the ruthenium sensitizers.	
<b>Figure 1-6</b> .....	<b>9</b>
Absorption spectrum of the N719 dye in ethanol featuring two MLCT bands.	
<b>Figure 1-7</b> .....	<b>10</b>
Schematic of operation of the dye-sensitized electrochemical photovoltaic cell.	
<b>Figure 2-1</b> .....	<b>15</b>
Scanning electron micrograph of a sintered mesoscopic TiO <sub>2</sub> film supported on an FTO glass.	
<b>Figure 2-2</b> .....	<b>17</b>
The nanowire dye-sensitized cell, based on a ZnO wire array.	
<b>Figure 2-3</b> .....	<b>19</b>
(a) Scheme of vertically oriented self-organized TiO <sub>2</sub> nanowire array grown on FTO, (b) top-view FESEM image, and (c) cross-sectional FESEM image.	

<b>Figure 2-4</b> .....	<b>21</b>
Integration of transparent nanotube array architecture into dye solar cell structure.	
<b>Figure 2-5</b> .....	<b>21</b>
Response time determined by open circuit photovoltage decay for a transparent TiO <sub>2</sub> nanotube-based DSSC as well as response times for a TiO <sub>2</sub> nanoparticle-based DSSC.	
<b>Figure 2-6</b> .....	<b>22</b>
Comparison of (a) transport and (b) recombination time constants for NT- and NP-based DSSCs as a function of the incident photon flux for 680 nm laser illumination.	
<b>Figure 2-7</b> .....	<b>23</b>
Comparison of the short-circuit photocurrent densities of dye-sensitized NT and NP cells as a function of film thickness.	
<b>Figure 2-8</b> .....	<b>24</b>
Cross-sectional SEM image of commercial AAO membrane pores coated with 20 nm of ZnO by ALD.	
<b>Figure 2-9</b> .....	<b>25</b>
I-V curve for the most efficient cell, 7 nm ZnO, under simulated AM1.5 illumination.	
<b>Figure 2-10</b> .....	<b>26</b>
Idealized two-dimensional cross section.	
<b>Figure 2-11</b> .....	<b>26</b>
Cross-sectional SEM image of a TiO <sub>2</sub> tube cleaved to reveal the i-ITO tube beneath. The concentric tubes, grown by atomic layer deposition, are embedded in a < 60 um long alumina pore.	

<b>Figure 2-12</b> .....	<b>27</b>
Schematic diagrams of the procedure used to fabricate the DSSCs.	
<b>Figure 2-13</b> .....	<b>29</b>
Scanning electron micrographs of quasi-ordered hollow TiO <sub>2</sub> hemispheres.	
<b>Figure 2-14</b> .....	<b>30</b>
Cross-sectional and top-view SEM images of a bilayer structure	
<b>Figure 2-15</b> .....	<b>31</b>
Incident-photon-to-current conversion efficiency (IPCE) spectra of DSSCs based on nanocrystalline TiO <sub>2</sub> films of ca. 6 μm thickness (1L) and ca. 12 μm thickness (2L) and the 1L-based bilayer structure having an overlayer of nano-embossed hollow sphere TiO <sub>2</sub> particles (1L-NeHS) and flat-surface submicrometer-sized TiO <sub>2</sub> particles (1L-CCIC).	
<b>Figure 2-16</b> .....	<b>33</b>
The scheme of novel architecture applied in DSSC electrode: self-organized hollow TiO <sub>2</sub> hemispheres under porous alumina with TiO <sub>2</sub> nanotubes inside.	
<b>Figure 3-1</b> .....	<b>35</b>
The fabrication process flow of various electrodes used in dye-sensitized solar cell.	
<b>Figure 3-2</b> .....	<b>37</b>
Schemes of the procedure of electrode synthesis.	
<b>Figure 3-3</b> .....	<b>39</b>
The schematic diagram of experimental setup for the aluminum electropolishing and anodization.	
<b>Figure 3-4</b> .....	<b>41</b>
Scheme of DSSC in the cross section.	
<b>Figure 4-1</b> .....	<b>45</b>

Anodization behavior of aluminum (500 nm) coated on various substrates as indicated.

**Figure 4-2**..... 46

Photographs show the FTO glass after anodization.

**Figure 4-3**..... 47

AFM image of a blank FTO glass without annealing.

**Figure 4-4**..... 48

AFM image of a blank FTO glass annealing temperature.

**Figure 4-5**..... 50

SEM image of self-organized TiO<sub>2</sub> hollow hemispheres under aluminum oxide

**Figure 4-6**..... 50

Top-view of SEM image of self-organized hollow TiO<sub>2</sub> hemispheres grew directly on FTO glass.

**Figure 4-7**..... 51

X-Ray diffraction pattern of self-organized hollow TiO<sub>2</sub> hemispheres.

**Figure 4-8**..... 52

Cross-sectional view of SEM image of self-organized hollow TiO<sub>2</sub> hemispheres.

**Figure 4-9**..... 53

Cross-sectional SEM image of TiO<sub>2</sub> nanotubes with AAO template.

**Figure 4-10**..... 54

Top-view of SEM image of TiO<sub>2</sub> nanotubes with AAO template.

**Figure 4-11**..... 55

SEM image of TiO<sub>2</sub> nanorods with AAO template.

**Figure 4-12**..... 57

X-Ray diffraction (XRD) pattern of TiO<sub>2</sub> nanotubes formed by sol-gel synthesis.

**Figure 4-13**..... 57

Cross-sectional SEM image of TiO<sub>2</sub> nanotubes treated by TiCl<sub>4</sub> for 5 min and repeated 3 times.

**Figure 4-14**..... 58

Cross-sectional SEM image of TiO<sub>2</sub> nanotubes treated by TiCl<sub>4</sub> for 5 min and repeated 5 times.

**Figure 4-15**..... 58

Top-view of SEM image of TiO<sub>2</sub> nanotubes after TiCl<sub>4</sub> treated.

**Figure 4-16**..... 60

Schematic diagram showing the principal steps of modification of the underlying titanium/alumina interface.

**Figure 4-17**..... 61

Schemes of the electrode structures applied in dye sensitized solar cells (DSSCs) under study.

**Figure 4-18**..... 64

Photocurrent density-voltage characteristics of the DSSCs.

**Figure 4-19**..... 67

Photocurrent density-voltage characteristics of the DSSCs.

